Biosensors and Bioelectronics 146 (2019) 111748

Contents lists available at ScienceDirect

Biosensors and Bioelectronics

journal homepage: http://www.elsevier.com/locate/bios

Flagella act as *Geobacter* biofilm scaffolds to stabilize biofilm and facilitate extracellular electron transfer

Xing Liu [a], Shiyan Zhuo [a], Xianyue Jing [a], Yong Yuan [b], Christopher Rensing [a], Shungui Zhou [a,*]

[a] *Fujian Provincial Key Laboratory of Soil Environmental Health and Regulation, College of Resources and Environment, Fujian Agriculture and Forestry University, Fuzhou, 350002, China*

[b] *School of Environmental Science and Engineering, Guangdong University of Technology, Guangzhou, 510006, China*

ARTICLE INFO

Keywords:
Electroactive biofilm
Flagella
Geobacter sulfurreducens
Extracellular electron transfer
Cytochrome filaments

ABSTRACT

Flagella are widely expressed in electroactive biofilms; however, their actual role is unknown. To understand the role of flagella, two *Geobacter sulfurreducens* strains (KN400 and PCA, with and without flagella, respectively) were selected. We restored flagellum expression *in trans* in strain PCA and prevented flagellum expression in strain KN400. Electrochemical results showed that flagellum restoration in strain PCA promoted current generation, while flagellum deletion in strain KN400 impaired current production. However, the expression of conductive pili and outer surface *c*-type cytochromes was not affected. Further microscopic analyses demonstrated that flagella promoted the formation of thicker biofilms and served as biofilm matrix scaffolds to accommodate more extracellular cytochromes with an orderly arrangement, which increased the electron diffusion rate within the biofilm. Our findings reveal an unprecedented structural role for flagella in stabilizing electroactive biofilms and highlight the importance of cytochromes in electron transfer across biofilms, which will deepen our understanding of biofilm conductivity.

1. Introduction

Electroactive bacteria can use electrodes as electron sources or sinks to support growth (Logan, 2009). They have been widely used in bioelectrochemical systems (BESs), such as microbial fuel cells for current generation and wastewater treatment, microbial electrolysis cells for high-value chemical production, and electrofermentation systems to tune microbial fermentative metabolisms (Logan, 2009; Logan and Regan, 2006). However, microbes do not exist in a single-cellular form on the electrode but usually form an electroactive biofilm tens of micrometers in thickness (Nevin et al., 2009; Reguera et al., 2006). This biofilm is electrically conductive, and electrons can be transported to the electrode via extracellular electron transfer (EET) (Malvankar et al., 2012). Previous studies on EET in electroactive biofilms mainly focused on the study of the model organism *Geobacter sulfurreducens,* which can often dominate the anode of microbial fuel cell (Jung and Regan, 2007; Kiely et al., 2011; Torres et al., 2009), is known as the most efficient electrogen (Nevin et al., 2008; Yi et al., 2009) and has a completely sequenced genome and well-established genetic system (Coppi et al., 2001).

G. sulfurreducens forms a thick electroactive biofilm on anodes. This biofilm is metabolically active even at the outer layer, but its thickness is limited (Bonanni et al., 2013; Franks et al., 2009). *c*-Type cytochromes and conductive pili are abundant in *Geobacter* biofilms (Nevin et al., 2009; Reguera et al., 2006; Stephen et al., 2014). In particular, they are important in EET for the growth of cells far from the anode. Interestingly, the distribution of cytochromes in electroactive biofilms is not irregular. For example, OmcZ is mainly distributed at the anode surface, and OmcB is mostly abundant in the outer layer of the biofilm (Inoue et al., 2011; Stephen et al., 2014). However, except the OmcZ, the extracellular cytochromes of OmcB, OmcS, OmcT and OmcE seems unnecessary for the current generation of *G. sulfurreducens* biofilm (Richter et al., 2009). Three models have been suggested for the EET in the *G. sulfurreducens* biofilm: (i) electron transfer along metallic-like conductive pili (Malvankar et al., 2011); (ii) an electron hopping mechanism involving electron exchange between cytochromes in the biofilm matrix (Snider et al., 2012; Strycharz-Glaven et al., 2011); and (iii) the mechanistic stratification in biofilms coordinately operated between conductive pili in the outer layer of the biofilm and cytochromes in the underlayer (Steidl et al., 2016). However, various factors will limit EET, especially the redox gradient across the biofilm formed by the uneven distribution of extracellular cytochromes (including loosely

---

* Corresponding author.
E-mail address: sgzhou@fafu.edu.cn (S. Zhou).

https://doi.org/10.1016/j.bios.2019.111748
Received 3 July 2019; Received in revised form 22 September 2019; Accepted 30 September 2019

bound outer-membrane cytochromes and cytochromes in the extracellular biofilm matrix) (Snider et al., 2012; Strycharz-Glaven et al., 2011), the rate of mass transport (protons or counter ions and acetate) through the biofilm (Bond et al., 2012) and the conductivity of pili (Liu et al., 2014; Vargas et al., 2013).

Flagella are widely expressed in *Geobacter* species. They usually are regarded as the motile organelle involved in chemotaxis toward Fe(III) oxides (Childers et al., 2002; Ueki et al., 2012). In addition, the motility of flagella can initiate the surface attachment of bacterial cells (Haznedaroglu et al., 2010) or promote the recruitment of planktonic cells, thus facilitating biofilm formation (Houry et al., 2010; Kerchove and Elimelech, 2008). However, flagellar motility is unnecessary once initial colonization is complete. It has been revealed that during biofilm development in other motile bacteria, for example *Bacillus* and *Pseudomonas*, the expression of motility-related genes was switched off during the motility-to-biofilm transition (Guttenplan and Kearns, 2013). Surprisingly, flagella are widely expressed in electroactive biofilms of *G. sulfurreducens* on inert anodes. Notably, flagella were shown to be nonconductive (Sure et al., 2016), and therefore should not contribute to the conductivity of the biofilm. The actual role of flagella in the cemented electroactive biofilm remains elusive.

To examine the role of flagella in the electroactive biofilm, two efficient current producers of *G. sulfurreducens*, the flagella-deficient strain PCA and flagella-containing strain KN400, were selected as control strains in this study. We also restored the expression of flagella in strain PCA and prevented the expression of flagella in strain KN400. All of these strains were tested for current generation, and the resulting biofilms were characterized. We observed that the expression of flagella increased the biofilm thickness and then enhanced the current generation by *G. sulfurreducens*. This can be credited to the structural role of flagella in the biofilm, which not only stabilized the biofilm to accommodate more cells but also increased the anchoring of extracellular cytochromes and facilitated the orderly arrangement of cytochromes in the biofilm matrix. Our results provide an unprecedented model of flagella involved in EET in the electroactive biofilm.

2. Materials and methods

2.1. Bacterial strains and culture conditions

The bacterial strains used in this study are listed in Supplementary Table S1. *Geobacter sulfurreducens* strain PCA (ATCC-51573) was received from ATCC, and *G. sulfurreducens* strain KN400 was provided by Prof. Derek Lovley. Both strains were routinely cultured in NBAF medium containing 40 mM fumarate as an electron acceptor as previously reported (Coppi et al., 2001). When performing the Fe(III) reduction test, FCA medium (56 mM ferric citrate as electron acceptor) was used as previously described (Liu et al., 2014). The concentration of produced Fe(II) was measured by the ferrozine assay. The chemically competent *E. coli* strain DH5α was used for routine cloning and was cultured at 37 °C in Luria-Bertani liquid medium or agar plates supplied with the appropriate antibiotics.

2.2. Mutant constructions

All primers used for mutant construction and verification are listed in Supplementary Table S2. To prevent the expression of flagella in strain KN400, the gene *filC* (KN_2978), which encodes the flagella structural protein, was replaced by a gentamycin cassette. Briefly, three DNA fragments were first prepared: the primer pairs flicUPf/flicUPr and filcDNf/filcDNr were used to amplify the sequences 500 bp upstream and downstream, respectively, of *filC*, using strain KN400 genomic DNA as a template, and the primer pair gentFor/gentRev was used to amplify the gentamycin resistance cassette from the plasmid pCM351. These three fragments were seamlessly connected and fused with linearized pUC19 plasmid, generating the plasmid pUC-*filC* using the In-Fusion HD Cloning Kit (Takara Biomedical Technology, Beijing, China) as previously reported (Liu et al., 2018). The plasmid was linearized with *ScaI* (New England BioLabs (NEB), MA, USA) and then translocated into electrocompetent *G. sulfurreducens* strain KN400 by electroporation.

To restore the expression of flagella in strain PCA, the expression plasmid pRG5-*fgrM* was constructed. Briefly, the primer pair pRGfgrMf and pRGfgrMr was used to amplify the *fgrM* gene (KN400_0269) using *G. sulfurreducens* strain KN400 genomic DNA as a template. This fragment was inserted into the linearized expression vector of pRG5, which was digested by *EcoRI* (NEB), with In-Fusion HD Enzyme (Takara). The final plasmid was concentrated and electroporated into electrocompetent *G. sulfurreducens* strain PCA, generating stain PCA-pRG5*fgrM*. The control strain, PCA-pRG5, was constructed in the same way but was transformed with empty pRG5 vector. All mutants were verified by PCR (Fig. S1) and sequencing.

2.3. SDS-PAGE, western blotting and heme staining analyses

Whole cell lysates were prepared from late-log-phase cells. The outer membrane proteins were separated from the cell surface by shearing cells with a blender at a low speed and then centrifuging the cells (Liu et al., 2018). Proteins in the supernatant were isolated and concentrated by filtration (3 kDa cutoff, Amicon Centrifugal Filter, Merck Millipore, MA, USA) as previously described (Liu et al., 2018). The extracellular proteins in the anode biofilm were extracted following a previously published method (Sun et al., 2012) with slight modification. Briefly, the anode biofilm was scraped and resuspended in 0.9% NaCl. An equal volume of 2% Na_2-EDTA in 0.9% NaCl (pH 7.0) was added and mixed well. The mixture was incubated at 4 °C for 3 h and then centrifuged at 5000×*g* at 4 °C for 20 min. The supernatant was collected and filtered through a 0.22 μm membrane filter. The filtrate was further concentrated with an Amicon Centrifugal Filter (3 kDa cutoff, Merck Millipore).

The concentrations of all protein samples were determined by bicinchoninic acid assay (Micro BCA Protein Assay Kit, Thermo Fisher Scientific, Waltham, MA, USA). An equal amount of protein was separated by SDS-PAGE using 12.5% Tris-tricine polyacrylamide gel (Amresco, Solon, OH, USA). For heme staining, dithiothreitol was omitted from the sampling buffer (Ye et al., 2018). Proteins were transferred from gel to polyvinylidene difluoride membrane using a Semi-Dry Blotting System (Tanon, Shanghai, China). The blotting membrane was blocked with 5% nonfat milk and then treated with anti-PilA rabbit polyclonal antibodies and anti-rabbit secondary antibody conjugated with horseradish peroxidase sequentially. The PilA band was detected by chemiluminescence (SuperSignal West Pico Kit, Thermo Fisher Scientific). The *c*-type cytochromes were specifically heme-stained with *N,N,N',N'*-tetramethylbenzidine as previously described (Liu et al., 2018; Thomas et al., 1976).

2.4. Bioelectrochemical system construction and operation

Two-chambered H-shaped bioelectrochemical reactors were constructed as previously described (Huang et al., 2018; Nevin et al., 2009). The electrolyte was anaerobic fresh water medium except for a final concentration of 10 mM acetate that was supplied in the anolyte as previously reported (Liu et al., 2019). The electrodes were made of polished graphite carbon plate with a dimension of 5.5 × 2 × 0.3 cm and were cleaned by ultrasonication in MilliQ water several times. A constant voltage of 0.3 V (vs. Ag/AgCl) was applied to the working electrode, which served as an electron acceptor (Liu et al., 2014). Both chambers were kept anaerobically by purging with N_2–CO_2 (80/20) continually. The same amount of cells were inoculated into the anode chamber. When the OD600 reached ca. 0.2, the analyte was replaced with fresh analyte and the anode chamber was switched to a continuous flow through mode in which the fresh analyte was flowed through the chamber at a dilution rate of 0.15/h as previously described (Nevin et al., 2009). The current was recorded continuously with an electrochemical workstation (CHI 1000C, CH Instruments, Shanghai, China). Cyclic voltammetry was performed *in situ* under nonturnover conditions using CHI660D (CH Instruments) by scanning the biofilm electrode from 0.3 to −0.6 V.

2.5. Microscopy and ultraviolet–visible spectroscopy analyses

The expression of flagella in cells was examined under a transmission electron microscope. Cell cultures were directly applied to carbon-coated copper grids for 5 min. The grid was wiped with filter paper and negatively stained with 2% uranyl acetate. To analyze the distribution of cytochromes in the anode biofilm, the anode was heme-stained with 3,3'-diaminobenzidine (DAB) and embedded as previously described (McGlynn et al., 2015). The embedded anode was ultrathin sectioned and poststained with 1% $NaAuCl_4$, which intensified the electron density of DAB. The control experiment was performed in the same way except without the addition of H_2O_2 (Fig. S5). Samples were applied to grids and examined under a transmission electron microscope (TEM) operating at 100 kV (Tecnai T12, Thermo Fisher Scientific).

To prepare samples for scanning electron microscope examination, the anode was washed once with 0.01 M PBS (pH 7.2) and then immersed in 0.01 M PBS containing 2% glutaraldehyde for fixation at 4 °C overnight. The anode was washed again with 0.01 M PBS and dehydrated with an ethanol gradient. Finally, the anode was dried with critical point drying to minimize the artifact arising from the drying steps. Samples were sputtered with gold and examined under a scanning electron microscope (SU3500, Hitachi, Tokyo, Japan).

The cytochrome content in the anode biofilm was measured by redox difference spectroscopy using a UV–Vis Spectrophotometer (UV-2600, Shimadzu, Kyoto, Japan) as previously described (Steidl et al., 2016). The ultraviolet–visible spectra (from 350 to 650 nm) of oxidized and reduced (treated by sodium dithionite) extracellular cytochromes were obtained (Fig. S4). The amount of cytochromes was calculated by comparing the difference between the reduced and oxidized spectra at 552 nm (the α-Soret band) (Nakamura et al., 2009; Rollefson et al., 2011).

3. Results

3.1. Construction of flagellum-expressing and flagellum-non-expressing mutants

Two strains of *G. sulfurreducens* PCA and KN400 were selected considering that they are efficient in current production and can form thick biofilms on the anode (Reguera et al., 2006; Yi et al., 2009). Even though these two strains have different genetic background, they share similar mechanism for extracellular electron transfer to respire extracellular electron acceptors (Malvankar et al., 2012; Strycharz et al.,

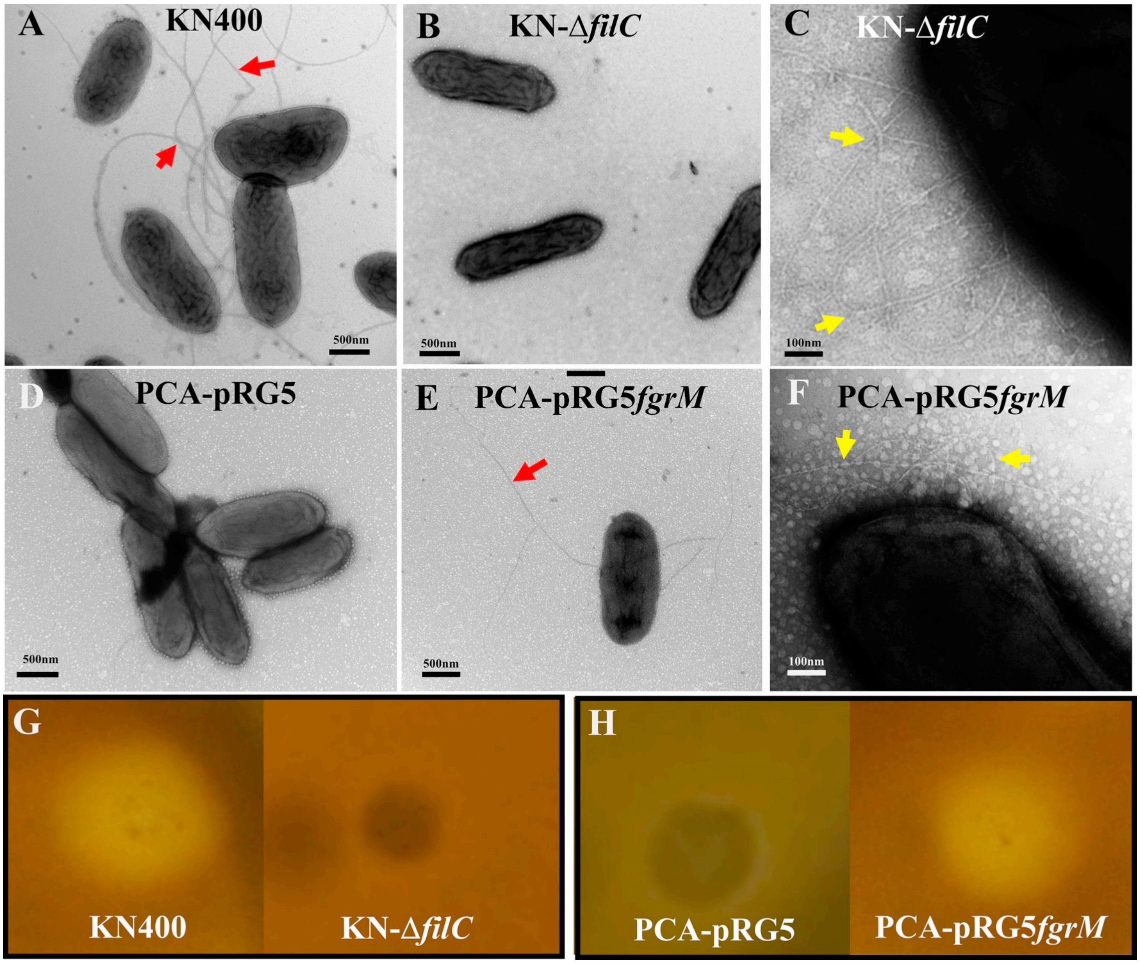

Fig. 1. Expression of flagella in *Geobacter sulfurreducens*. Representative transmission electron microscope images of *G. sulfurreducens* strain KN400 (A), the flagellar gene deletion strain of KN-Δ*filC* (B, C), strain PCA-pRG5 carrying the empty expression vector of pRG5 (D), and strain PCA-pRG5*fgrM* expression of *fgrM in trans* (E, F). The red and yellow arrows indicate flagellum and pilus, respectively. (G, H) Swimming motility test on ferric citrate agar (0.3%) plate. Deletion of *filC* prevented the expression of flagella in strain KN400 and inhibited its motility but did not affect the expression of pili. Expression of *fgrM in trans* in strain PCA-pRG5 recovered the expression of flagella and promoted motility. (For interpretation of the references to colour in this figure legend, the reader is referred to the Web version of this article.)

2011). Flagellum is much thicker than pilus and it is easier to distinguish flagellum from pilus by transmission electron microscopy (Ueki et al., 2012; Yi et al., 2009). *G. sulfurreducens* strain KN400 expressed both pili and flagella (Fig. 1A, C). In contrast, *G. sulfurreducens* strain PCA only expressed pili even though it had an intact flagellin synthesis and assembly machinery (Ueki et al., 2012). A previous study demonstrated that the insertion of a transposon in the master transcriptional regulator gene *fgrM* prevented the expression of flagella in strain PCA (Fig. 1D) (Ueki et al., 2012). FgrM is a RpoN-dependent enhancer-binding protein and has been shown to be essential for the synthesis of flagella. Therefore, the expression of flagella in *G. sulfurreducens* strain PCA was restored by expressing *fgrM in trans* on the expression plasmid pRG5-*fgrM*, generating *G. sulfurreducens* strain PCA-pRG5*fgrM*. Both flagella and pili were normally expressed and assembled in *G. sulfurreducens* strain PCA-pRG5*fgrM* (Fig. 1E and F). Correspondingly, to abolish the expression of flagella in *G. sulfurreducens* strain KN400, *filC,* which encodes a flagellar filament structural protein synthase, was deleted, generating *G. sulfurreducens* strain KN-Δ*filC* which could not express flagella but could express pili normally (Fig. 1B and C). A control strain of *G. sulfurreducens* strain PCA-pRG5 carrying an empty pRG5 vector was also generated.

The expression of flagella contributes to the motility of bacterial species. Swimming motility was tested on soft agar plates to verify the functional expression of flagella in the *G. sulfurreducens* strains(Ueki et al., 2012). A drop of culture cell was applied on the FCA agar, and a larger clear Fe(III) reduction zone around cells indicated the efficient mobility of the cell(Ueki et al., 2012). *G. sulfurreducens* strain KN400 was motile on FCA agar plates with a transparent Fe(III) reduction circle, but *G. sulfurreducens* strain PCA-pRG5 was nonmotile (Fig. 1G and H). As expected, the deletion of *filC* abolished the motility of strain KN400 (Fig. 1G), and the functional expression of FgrM restored the motility of *G. sulfurreducens* strain PCA (Fig. 1H).

3.2. The expression of flagella promotes current generation

The effect of the expression of flagella on the current generation of *G. sulfurreducens* was tested in a three-electrode microbial fuel cell. Wild-type *G. sulfurreducens* strain KN400 produced a maximum current density of approximately $1.24 \pm 0.035\,\text{mA/cm}^2$ in 62 h, while strain KN-Δ*filC* generated a lower maximum current of approximately $0.91 \pm 0.01\,\text{mA/cm}^2$ in 78 h (Figs. 2A and 3A). Similarly, *G. sulfurreducens* strain PCA-pRG5*fgrM* produced a current with a maximum of $0.54 \pm 0.005\,\text{mA/cm}^2$ in 99 h, which was more efficient than strain PCA-pRG5, generating a maximum current of $0.37 \pm 0.012\,\text{mA/cm}^2$ in 146 h (Figs. 2B and 3A). Previous studies on the function of flagella in the formation of biofilms indicated that the flagella promoted the attachment and residence of bacteria on surfaces to initiate biofilm formation (Haznedaroglu et al., 2010; Houry et al., 2010; Kerchove and Elimelech, 2008). Here, we showed that the expression of flagella accelerated the start of current generation in *G. sulfurreducens* strains, which displayed an increase of 26% for strain KN400 and 47% for strain PCA, indicating that flagella could also accelerate the formation of the electroactive biofilm on the anode.

To rule out pleiotropic effects of flagellum expression on the metabolism of all tested *G. sulfurreducens* strains, the reduction of ferric citrate, which is reduced on the outer cell surface (Gaspard et al., 1998; Liu et al., 2014; Seeliger et al., 1998), was further examined. Unsurprisingly, *G. sulfurreducens* strain KN-Δ*filC* and strain PCA-pRG5*fgrM* showed a comparable Fe(III) reduction rate when compared with the control strains of *G. sulfurreducens* strain KN400 and strain PCA-pRG5, respectively (Fig. 3F), indicating a similar ability to transfer electrons to the outer cell surface between the mutant and control strains. In particular, strain KN400 had a higher metabolism than strain PCA (Fig. 3F), which is consistent with the previous report (Yi et al., 2009).

The expression of conductive filaments of pili can promote the current generation of *G. sulfurreducens* (Liu et al. 2014; Reguera et al. 2006; Vargas et al. 2013). In particular, *G. sulfurreducens* strain KN400 grow many more conductive pili than strain PCA and produces twice the current that strain PCA produced (Yi et al., 2009). In contrast, flagella are nonconductive. The observation that the expression of flagella also promoted current generation in *G. sulfurreducens* implied that nonconductive flagella could also participate or facilitate the EET for anode reduction in electroactive biofilms.

3.3. Flagellum expression contributes to a thicker anodic biofilm with higher bacterial and cytochrome loads

After initial colonization, *G. sulfurreducens* cells continuously grow to form a metabolically active biofilm on the anode and generate current until a maximum value is reached (Marsili et al., 2010). After that, the current will decrease slowly as cells gradually die inside the biofilm (Dhar et al., 2017; Sun et al., 2015). However, the thickness of the biofilm will still increase and can be over one hundred micrometers due to the accumulation of dead cells in the inner layer and the growth of cells in the outer layer of the biofilm (Robuschi et al., 2013; Sun et al., 2015). Considering this, the anodic biofilms from different

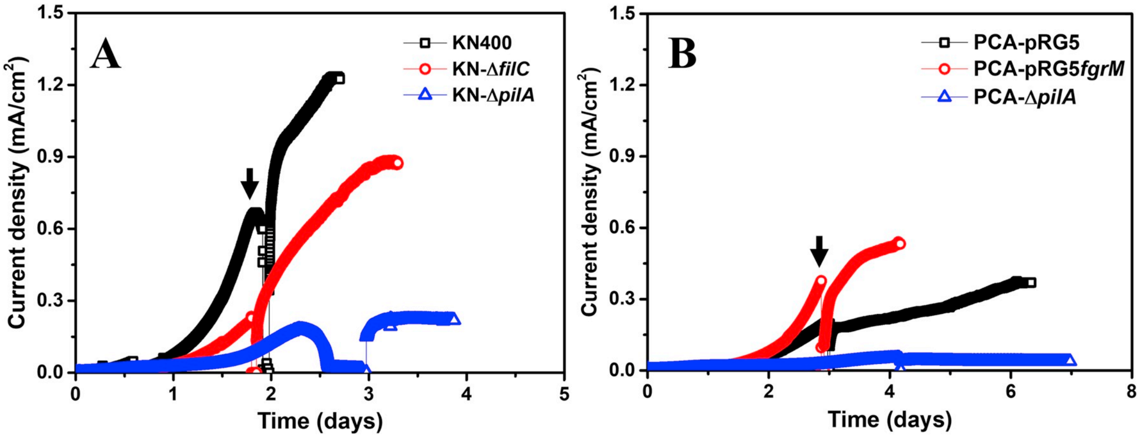

Fig. 2. Current generation. (A) Representative current production of different KN400 strains. (B) Representative current production of different PCA strains. Five biological replicates were performed for each strain. The expression of flagella promoted current generation. The black arrow indicates medium exchange, and the systems were switched to a continuous flow through mode at a dilution rate of 0.15/h. *G. sulfurreducens* strain KN-Δ*pilA* and *G. sulfurreducens* strain PCA-Δ*pilA* are the pili deficient strains of *G. sulfurreducens* KN400 and *G. sulfurreducens* PCA, respectively, both of which were deficient in current generation and acted as negative controls.

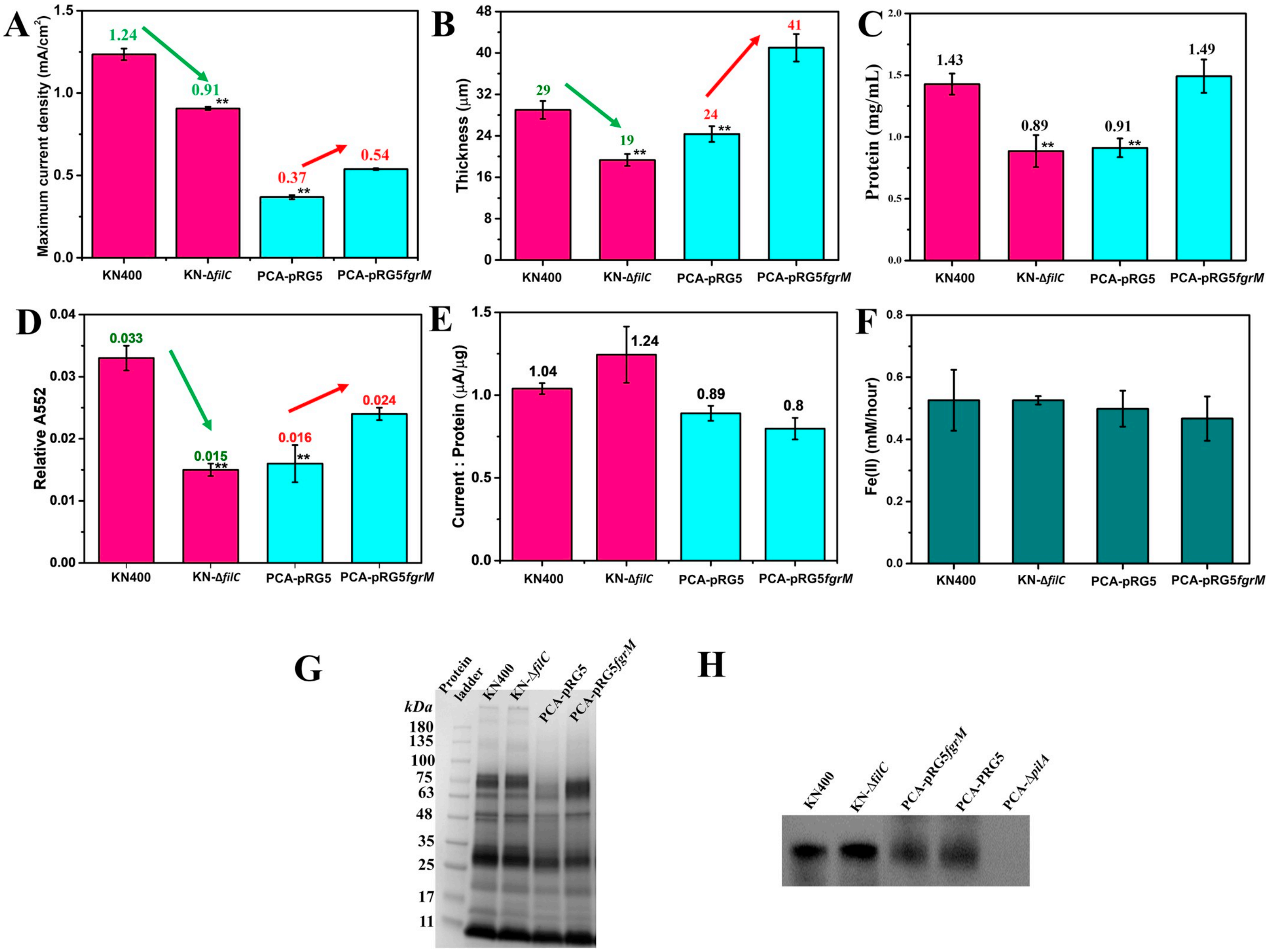

Fig. 3. Anode biofilm characterization. (A) Static calculations of the maximum currents produced from different *G. sulfurreducens* strains. (B) Static calculations of anode biofilm thicknesses from different *G. sulfurreducens* strains. The thickness was calculated from the confocal images of the anodic biofilm. (C) Quantification of total proteins in anode biofilm. Cells were scraped from the anode and resuspended in 5 mL PBS. Cells were lysed by sonication. (D) Static calculations of the relative amount of cytochromes in the anode biofilm from *G. sulfurreducens* strains. (E) Normalized current generation per unit of protein. (F) Ferric citrate reduction test. The averaged reduction rates were calculated. (G) Heme staining of SDS-PAGE gel of extracellular *c*-type cytochromes from anode biofilm matrix. (H) Western blotting analysis of PilA expression in different *G. sulfurreducens* strains. Data were collected from five biological replicates and presented as the mean ± standard deviation (**$p < 0.01$).

G. sulfurreducens strains producing a maximum current were selected and further characterized to provide a consistent comparison between the different strains and published data. A thick *G. sulfurreducens* biofilm usually produces a high current (Liu et al., 2014). Consistent with the current produced, *G. sulfurreducens* strain KN-Δ*filC* formed a thinner biofilm than strain KN400, with the thickness being reduced from 29 ± 1.73 μm to 19 ± 1.15 μm (Fig. 3B). In contrast, *G. sulfurreducens* strain PCA-pRG5*fgrM* grew a thicker biofilm than strain PCA-pRG5, increasing from 24 ± 1.53 μm to 41 ± 2.65 μm (Fig. 3B). In particular, all biofilms were metabolically active and had a compact structure (Fig. S3), which is typical of electroactive biofilms (Nevin et al., 2009). These data indicated that the expression of flagella in *G. sulfurreducens* could further stabilize the biofilm and facilitate the formation of a thicker anodic biofilm with a higher bacterial load (Fig. 3C). The current generation per cell in the biofilm was further estimated by calculating the electron transfer rate per unit of protein at the maximum current (Fig. 3E). As previously reported*,* *G. sulfurreducens* strain KN400 was more efficient in current generation than strain PCA on a per cell basis (Fig. 3E) (Yi et al., 2009). Notably, the restoration or deletion of flagella in *G. sulfurreducens* did not affected the electrogenic activity of single cells (Fig. 3E). These data indicated that the current increase in flagella-restored strain PCA and the current decrease in flagella-deleted strain KN400 were due to a higher bacterial load on the anode of strain PCA-pRG5*fgrm* and a lower bacterial load on the anode of strain KN-Δ*filC*, respectively.

Both *c*-type cytochromes and conductive pili are important in EET of *G. sulfurreducens*. Outer surface cytochromes facilitate the electron transfer in the biofilm matrix, and conductive pili also contribute to the electron transfer pathway in EET for current generation. In particular, the hyperpiliated strain of *G. sulfurreducens* produces a higher current than the wild-type strain, even though it does not form a thicker biofilm (Leang et al., 2013). The expression of *c*-type cytochromes and pili was examined to identify their contribution to the generation of a higher current in flagella-expressing *G. sulfurreducens* strains. The cytochrome contents in different anode biofilms were measured by redox difference spectroscopy. The biofilm of strain KN-Δ*filC* had a lower cytochrome load than the biofilm generated by strain KN400 (Fig. 3D). In contrast, the biofilm of *G. sulfurreducens* strain PCA-pRG5*fgrM* contained more cytochromes than the biofilm of strain PCA-pRG5 (Fig. 3D). It is not surprising that the expression of flagella did not affect the excretion of *c*-type cytochromes (Figs. 3G and S2) and that a thicker biofilm could accommodate more extracellular cytochromes. Particularly, the extracellular cytochrome profiles of biofilms between *G. sulfurreducens* strain KN400 and strain KN-Δ*filC* and between *G. sulfurreducens* strain PCA-pRG5 and strain PCA-pRG5*fgrM* were similar with a slightly stronger band (with a molecular weight ca. 75 kDa) in the preparation from strain PCA-pRG5*fgrM* (Fig. 3G). In addition, *G. sulfurreducens* strain KN-Δ*filC* showed a comparable pili expression to strain KN400 (Fig. 3H), which was also the case between *G. sulfurreducens* strain PCA-pRG5*fgrM* and strain PCA-pRG5 (Fig. 3H). All these data indicated that the increase in current after the expression of flagella was positively correlated with biofilm thickness and the load of outer membrane *c*-type cytochromes in the anodic biofilm matrix.

3.4. Flagella serve as scaffolds of electroactive biofilms and promote the formation of cytochrome filaments

Flagella usually act as motile organelles to accelerate the attachment of bacteria on surfaces to initiate biofilm formation. Recently, Serra et al. discovered that flagella in nonconductive *Escherichia coli* biofilms serve a structural role (Serra et al., 2013). They found the flagella wrapped around cells and thus played a role in cementing cells together, similar to polysaccharides (Serra et al., 2013). The distribution of flagella in the *G. sulfurreducens* anodic biofilm was characterized. As shown in Fig. 4A and B, no flagella were observed in the *G. sulfurreducens* strain PCA-pRG5 biofilm. In contrast, flagella were abundant in the PCA-pRG5*fgrM* biofilm (Fig. 4D and E). As indicated, cells were cross-linked by flagella, which in turn formed scaffolds to accommodate cells (Fig. 4D and E) a similar role as the structural function of pili in the anode biofilm (Reguera et al., 2007). In the presence of heme-containing proteins, DAB can be oxidized by hydrogen peroxide, thus forming a dark brown precipitate with a high electron opacity. In this regard, the distribution of cytochromes in the biofilm matrix was visualized after treating the biofilm with DAB in the presence or absence of H_2O_2. As indicated in the TEM images (Figs. 4C and S6A), cytochromes were dispersed in the biofilm matrix of *G. sulfurreducens* strain PCA-pRG5 and strain KN-Δ*filC* arbitrarily. Surprisingly, cytochromes in the *G. sulfurreducens* strain PCA-pRG5*fgrM* and strain KN400 biofilm matrix had an orderly arrangement, forming cytochrome filaments to connect cells, and were distributed throughout the biofilm (Figs. 4F, S5B, S6B), which could not be detected in the absence of H_2O_2 and might benefit the long-distance electron transfer in the biofilm.

To further analyze the electron transfer across the biofilm matrix, cyclic voltammograms (CVs) of the biofilms were scanned under non-turnover conditions (acetate depleted). Fig. 5A shows the typical CVs obtained from the biofilms of *G. sulfurreducens* PCA-pRG5 and strain PCA-pRG5*fgrM*. Two major redox peaks with formal potentials of −0.376 V and −0.306 V were observed in the CVs of these two biofilms, which are the same as the reported PCA biofilm (Fricke et al., 2008). The almost identical CV characterizations of these two biofilms further suggested that the electrochemical activities of the outer surface cytochromes of PCA were not affected by the expression of flagella. The CVs of *G. sulfurreducens* strain KN400 and strain KN-Δ*filC* biofilm also showed similar characteristics (Fig. 5B), indicating that cytochromes of KN400 were also not affected by the flagellum deletion. The electron transfer inside the *Geobacter* biofilm showed a diffusive behavior (Bonanni et al., 2012; Snider et al., 2012; Strycharz-Glaven et al., 2011). The electrochemical kinetics of the biofilms in terms of the electron diffusivity were analyzed by performing cyclic voltammetry at different scan rates under nonturnover condition (Fig. S7). The slope of the linear

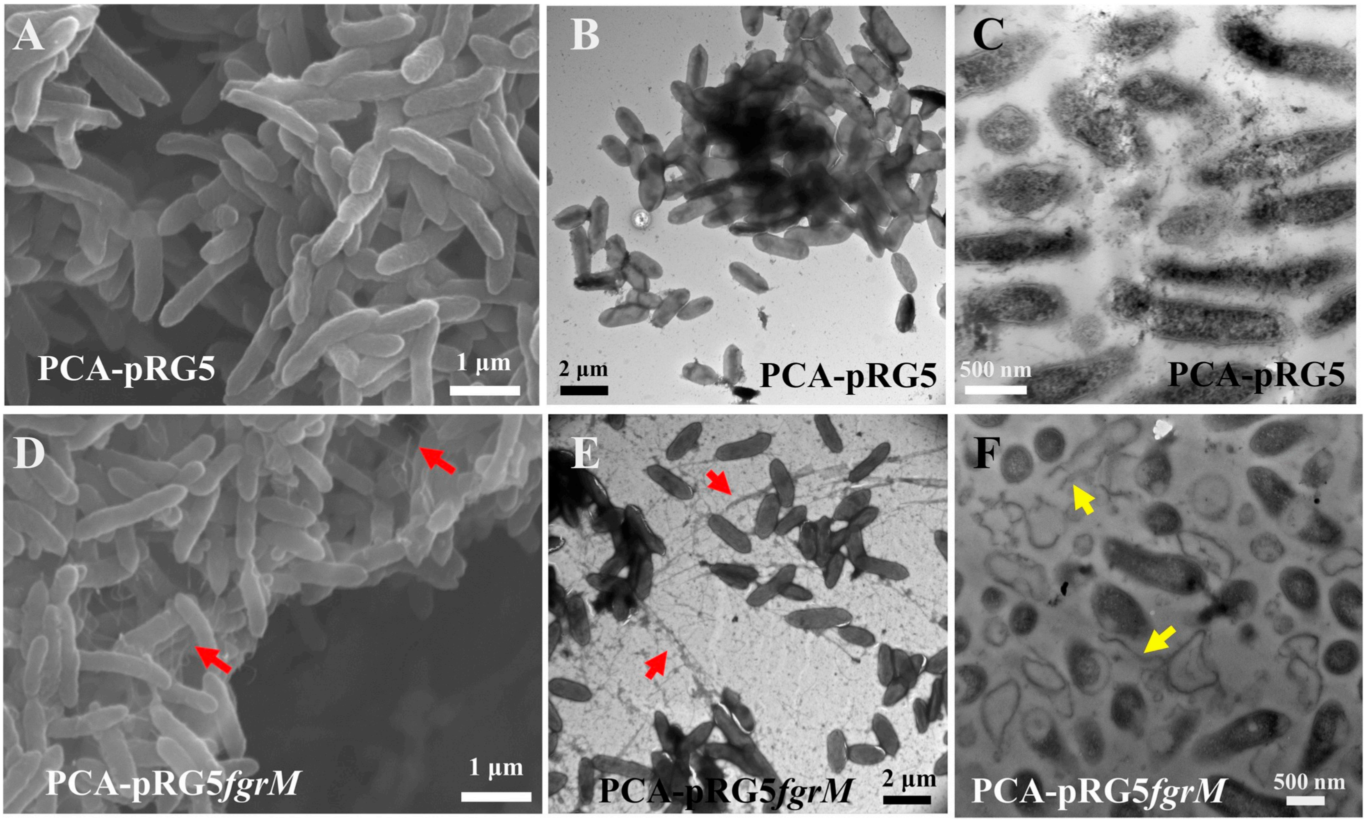

Fig. 4. Electron microscope images of anode biofilm from *G. sulfurreducens* strains. (A, D) Representative scanning electron microscope images of anode biofilm of strain PCA-pRG5 and PCA-pRG5*fgrM* from 35 images and 31 images, respectively. (B, E) Representative transmission electron microscope images of whole cell mounts collected from the anode biofilm of strain PCA-pRG5 and PCA-pRG5*fgrM* from 41 images and 27 images, respectively. The red arrows indicate the flagella. (C, F) Representative transmission electron microscope images of thin sections of the anode biofilm of strain PCA-pRG5 and PCA-pRG5*fgrM* from 56 images treated with DAB and H_2O_2 sequentially. The yellow arrows indicate heme-containing filaments. (For interpretation of the references to colour in this figure legend, the reader is referred to the Web version of this article.)

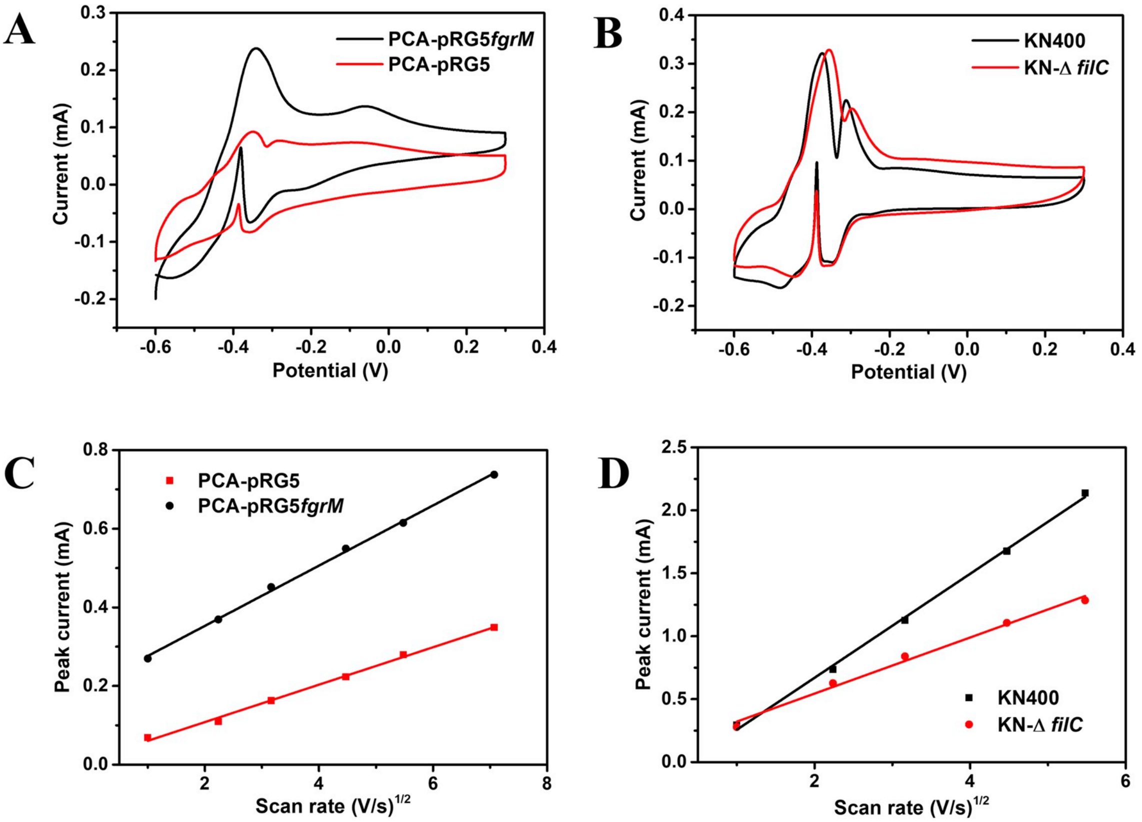

Fig. 5. Cyclic voltammetry of anodic biofilm. Cyclic voltammograms under nonturnover conditions for *G. sulfurreducens* biofilms at a scan rate of 1 mV/s for *G. sulfurreducens* strain PCA-pRG5 and strain PCA-pRG5*fgrM* (A), and for *G. sulfurreducens* strain KN400 and strain KN-Δ*filC* (B). Linear dependence of baseline-subtracted oxidation peak current height with the square root of the scan rate: (C) *G. sulfurreducens* strain PCA-pRG5 and strain PCA-pRG5*fgrM*, with slopes of 0.048 and 0.077 respectively. (D) *G. sulfurreducens* strain KN400 and strain KN-Δ*filC*, with slopes of 0.413 and 0.222 respectively. The baseline-subtracted anodic peak current at −0.35 V was extracted for calculation.

regression with the baseline-subtracted peak currents against the square root of the scan rate was calculated (Fig. 5C and D) to estimate the electron diffusivity using the Randles-Sevcik Equation as previously reported (Katuri et al., 2012), and the total amount of charge carriers in the biofilm matrix was estimated from the area of peaks on CVs at the 1 mV/s scan rate. An electron diffusivity of 3.7×10^{-6} and 1.6×10^{-6} could be estimated for the biofilm of *G. sulfurreducens* strain KN400 and strain KN-Δ*filC*, respectively, and an electron diffusivity of 1.7×10^{-6} and 2.1×10^{-6} for *G. sulfurreducens* strain PCA-pRG5 and strain PCA-pRG5*fgrM*, respectively. The higher electron diffusivity represented a higher biofilm conductivity. The results suggested that the expression of flagella increased the electron diffusivity within the *Geobacter* biofilm.

4. Discussion

Our results demonstrated an unprecedented structural role of flagella in building *Geobacter* biofilms, promoting biofilm conductivity and enhancing current generation. We showed that the expression of flagella in *G. sulfurreducens* not only stabilized the anodic biofilm, promoting the formation of a thicker biofilm with more cells and cytochromes accommodated, but also facilitated the orderly arrangement of extracellular cytochromes in the biofilm matrix, which increased the electron

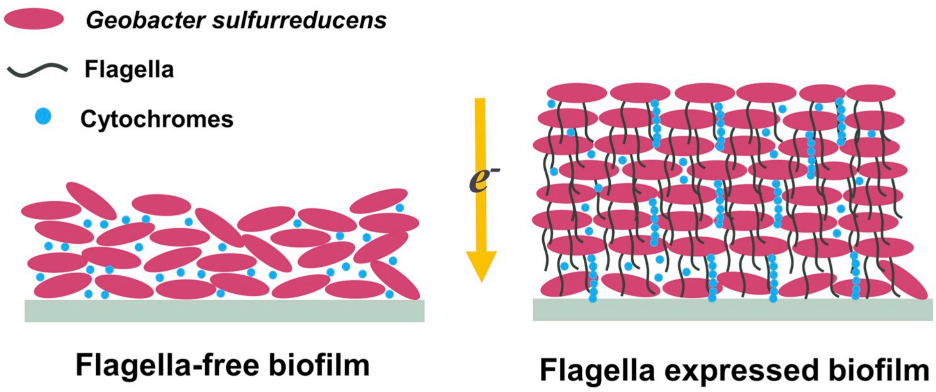

Fig. 6. Model of flagella in EET of a *G. sulfurreducens* biofilm. The expression of flagella in *G. sulfurreducens* promoted the formation of a thicker anodic biofilm accommodating more bacterial cells and extracellular cytochromes with an orderly arrangement which increased the electron diffusion rate and enhanced current generation.

diffusion rate (Fig. 6).

We have shown that the expression of flagella accelerated the initiation of current generation. This derives from the motility function of flagella as the initial colonization of the anode is generated by planktonic cells (Marsili et al., 2010). After early phases of colonization, these initially attached cells generate new cells continuously, thereby constructing the anodic biofilm (Marsili et al., 2010). However, the thickness of anodic *G. sulfurreducens* biofilms is finite and is determined by various factors(Bonanni et al. 2012, 2013; Bond et al., 2012; Liu et al., 2010; Torres et al., 2008). Previous reports on the *G. sulfurreducens* anodic biofilm indicated that the nutrition availability and the diffusion rate of protons or counter ions inside the biofilm restricted the formation of thicker anodic biofilms (Bonanni et al., 2012; Bond et al., 2012; Liu et al., 2010; Torres et al., 2008). However, these should not be the major limiting factors for the formation of a thicker biofilm in our system as a bicarbonate buffering system was used as the electrolyte with constant agitation and a high concentration of acetate was supplied continuously (Bonanni et al., 2013), both of which supported the increase in the anodic biofilm thickness of *G. sulfurreducens* after flagellar expression. More recent studies indicated that the redox gradient across biofilms, with increasingly more oxidized cytochromes from the outer layer biofilm to the surface of the anode, dominated and contributed to the limited thickness of anodic biofilms (Bonanni et al., 2013; Robuschi et al., 2013; Strycharz-Glaven et al., 2011). The close distribution of electroactive moieties is necessary for efficient electron diffusion (Cordes and Giese, 2009). In our study, the additional biofilm thickness increase after expression of flagella should be credited to the higher expressed and orderly arranged cytochromes, which increased the rate of electron diffusion and then alleviated the thickness limitation. Notably, how flagella affected the distribution of cytochromes in electroactive biofilms was not determined in this study. Previous studies have suggested that extracellular cytochromes can distribute regularly in anodic biofilms (Inoue et al., 2011; Stephen et al., 2014). For example, OmcZ was mainly distributed at the interface between *G. sulfurreducens* and the anode and was regulated by unknown mechanisms even though the expression of OmcZ was the same throughout the biofilm (Franks et al., 2012; Inoue et al., 2011). The cytochrome filaments in the flagella-expressing biofilms were not from the cytochromes on the outer membrane (Figs. 4F and S6B) or on the pili as the cytochrome filaments were not detected in pili-expressing but flagella-free biofilms (Figs. 4C and S6A). In addition, cytochromes should not be attached to the flagella. A recent study suggested that extracellular cytochromes could self-assemble to form filaments (Wang et al., 2019). Considering that there were abundant cytochromes in the biofilm matrix, the expression of flagella might promote the self-assembly of cytochromes in anodic biofilms, and future work is warranted.

The finding that the expression of flagella increased the biofilm conductivity deepens the understanding of the EET of electroactive biofilms. Previous studies on *G. sulfurreducens* biofilms have demonstrated both a conductive function and a structural role of pili in biofilm formation (Reguera et al., 2007). In particular, the expression of conductive pili is necessary for EET and contributes the biofilm conductivity (Malvankar et al., 2011). However, further increases in pili conductivity in *G. sulfurreducens* neither increased the biofilm thickness nor promoted the current generation (Tan et al., 2017). In addition, inducing the excessive expression of pili in *G. sulfurreducens* could not further increase the thickness of the biofilm (Leang et al., 2013). These results suggested that conductive pili played a limited structural role in the formation of the electroactive biofilm and had a limited effect on the EET as their excessive expression could not further stabilize the biofilm and thus increase the biofilm thickness. In contrast, in our study, the expression of nonconductive flagella further increased the biofilm thickness and induced the orderly arrangement of extracellular cytochromes. As a result, the flagella-abundant biofilms produced a significantly higher current than flagella-absent biofilms. Therefore, this discovery highlights the structural role of flagella and the importance of cytochromes for EET in electroactive biofilms. However, we did not exclude the pili that also participated in the extracellular electron transfer in the flagella-expressing biofilm. To dissect the function of pili in flagella-expressing biofilms, preventing the expression of pili in flagella-expressing *G. sulfurreducens* strains is warranted.

5. Conclusion

In summary, the present study, for the first time, focused on the potential role of flagella in the formation and EET capability of biofilms. The results showed that flagella were widely expressed in anodic biofilms, whose expression stimulated biofilm formation, stabilized the biofilm to accommodate more bacterial cells and promoted current density in the BESs. Microscopic and electrochemical measurements confirmed that flagella could act as biofilm matrix scaffolds to accommodate more extracellular cytochromes with an orderly arrangement and thus increase the electron diffusion rate within the biofilms, showing that the induced flagella were linked to biofilm conductivity. Therefore, inducing the expression of flagella in electroactive bacteria should be an alternative strategy to construct high-efficiency electroactive biofilms for bioelectrochemical systems. It is worth noting that the increase in biofilm thickness also increases environmental stress inside the biofilm, such as acid accumulation and substrate shortage, which in turn reduces the cell vitality and EET capacity (Babauta et al., 2012; Franks et al., 2009; Renslow et al., 2013; Sun et al., 2015). Meanwhile, the findings of this study will have important implications for an in-depth understanding of the extracellular electron transfer process of electroactive biofilms.

Declaration of competing interest

The authors declare that they have no known competing financial interests or personal relationships that could have appeared to influence the work reported in this paper.

CRediT authorship contribution statement

Xing Liu: Data curation, Formal analysis, Funding acquisition, Methodology, Project administration, Supervision, Validation, Writing - original draft. **Shiyan Zhuo:** Data curation, Investigation. **Xianyue Jing:** Validation, Visualization. **Yong Yuan:** Writing - review & editing. **Christopher Rensing:** Writing - review & editing. **Shungui Zhou:** Project administration, Supervision, Writing - review & editing.

Acknowledgments

We sincerely thank Prof. Derek Lovley of the University of Massachusetts, Amherst for providing the *Geobacter sulfurreducens* strain KN400. This research was supported by the National Natural Science Foundation of China (31600089 and 41671264) and the National Postdoctoral Science Foundation (2017M622040).

Appendix A. Supplementary data

Supplementary data to this article can be found online at https://doi.org/10.1016/j.bios.2019.111748.

References

Babauta, J.T., Nguyen, H.D., Harrington, T.D., Renslow, R., Beyenal, H., 2012. pH, redox potential and local biofilm potential microenvironments within *Geobacter sulfurreducens* biofilms and their roles in electron transfer. Biotechnol. Bioeng. 109 (10), 2651–2662.

Bonanni, P.S., Bradley, D.F., Schrott, G.D., Busalmen, J.P., 2013. Limitations for current production in *Geobacter sulfurreducens* biofilms. ChemSusChem 6 (4), 711–720.

Bonanni, P.S., Schrott, G.D., Robuschi, L., Busalmen, J.P., 2012. Charge accumulation and electron transfer kinetics in *Geobacter sulfurreducens* biofilms. Energy Environ. Sci. 5 (3), 6188–6195.

Bond, D.R., Strycharz-Glaven, S.M., Tender, L.M., Torres, C.I., 2012. On electron transport through *Geobacter* biofilms. ChemSusChem 5 (6), 1099–1105.

Childers, S.E., Ciufo, S., Lovley, D.R., 2002. *Geobacter metallireducens* accesses insoluble Fe(iii) oxide by chemotaxis. Nature 416 (6882), 767–769.

Coppi, M.V., Leang, C., Sandler, S.J., Lovley, D.R., 2001. Development of a genetic system for *Geobacter sulfurreducens*. Appl. Environ. Microbiol. 67 (7), 3180–3187.

Cordes, M., Giese, B., 2009. Electron transfer in peptides and proteins. Chem. Soc. Rev. 38 (4), 892–901.

Dhar, B.R., Sim, J., Ryu, H., Ren, H., Santo Domingo, J.W., Chae, J., Lee, H.-S., 2017. Microbial activity influences electrical conductivity of biofilm anode. Water Res. 127, 230–238.

Franks, A.E., Glaven, R.H., Lovley, D.R., 2012. Real-time spatial gene expression analysis within current-producing biofilms. ChemSusChem 5 (6), 1092–1098.

Franks, A.E., Nevin, K.P., Glaven, R.H., Lovley, D.R., 2009. Microtoming coupled to microarray analysis to evaluate the spatial metabolic status of *Geobacter sulfurreducens* biofilms. ISME J. 4 (4), 509–519.

Fricke, K., Harnisch, F., Schröder, U., 2008. On the use of cyclic voltammetry for the study of anodic electron transfer in microbial fuel cells. Energy Environ. Sci. 1 (1), 144–147.

Gaspard, S., Vazquez, F., Holliger, C., 1998. Localization and solubilization of the iron (III) reductase of *Geobacter sulfurreducens*. Appl. Environ. Microbiol. 64 (9), 3188–3194.

Guttenplan, S.B., Kearns, D.B., 2013. Regulation of flagellar motility during biofilm formation. FEMS Microbiol. Rev. 37 (6), 849–871.

Haznedaroglu, B.Z., Zorlu, O., Hill, J.E., Walker, S.L., 2010. Identifying the role of flagella in the transport of motile and nonmotile *Salmonella enterica* serovars. Energy Environ. Sci. 44 (11), 4184–4190.

Houry, A., Briandet, R., Aymerich, S., Gohar, M., 2010. Involvement of motility and flagella in *Bacillus cereus* biofilm formation. Microbiology 156 (4), 1009–1018.

Huang, L., Tang, J., Chen, M., Liu, X., Zhou, S., 2018. Two modes of riboflavin-mediated extracellular electron transfer in *Geobacter uraniireducens*. Front. Microbiol. 9, 2886.

Inoue, K., Leang, C., Franks, A.E., Woodard, T.L., Nevin, K.P., Lovley, D.R., 2011. Specific localization of the c-type cytochrome OmcZ at the anode surface in current-producing biofilms of *Geobacter sulfurreducens*. Environ. Microbiol. Rep. 3 (2), 211–217.

Jung, S., Regan, J.M., 2007. Comparison of anode bacterial communities and performance in microbial fuel cells with different electron donors. Biotechnology Appl. Microbiol. Biotechnol. 77 (2), 393–402.

Katuri, K.P., Rengaraj, S., Kavanagh, P., O'Flaherty, V., Leech, D., 2012. Charge transport through *Geobacter sulfurreducens* biofilms grown on graphite rods. Langmuir 28 (20), 7904–7913.

Kerchove, A.J.d., Elimelech, M., 2008. Bacterial swimming motility enhances cell deposition and surface coverage. Environ. Sci. Technol. 42 (12), 4371–4377.

Kiely, P.D., Cusick, R., Call, D.F., Selembo, P.A., Regan, J.M., Logan, B.E., 2011. Anode microbial communities produced by changing from microbial fuel cell to microbial electrolysis cell operation using two different wastewaters. Bioresour. Technol. 102 (1), 388–394.

Leang, C., Malvankar, N.S., Franks, A.E., Nevin, K.P., Lovley, D.R., 2013. Engineering *Geobacter sulfurreducens* to produce a highly cohesive conductive matrix with enhanced capacity for current production. Energy Environ. Sci. 6 (6), 1901–1908.

Liu, X., Tremblay, P.-L., Malvankar, N.S., Nevin, K.P., Lovley, D.R., Vargas, M., 2014. A *Geobacter sulfurreducens* strain expressing *Pseudomonas aeruginosa* type IV pili localizes OmcS on pili but is deficient in Fe(III) oxide reduction and current production. Appl. Environ. Microbiol. 80 (3), 1219–1224.

Liu, X., Zhan, J., Jing, X., Zhou, S., Lovley, D.R., 2019. A pilin chaperone required for the expression of electrically conductive *Geobacter sulfurreducens* pili. Environ. Microbiol. 21 (7), 2511–2522.

Liu, X., Zhuo, S., Rensing, C., Zhou, S., 2018. Syntrophic growth with direct interspecies electron transfer between pili-free *Geobacter* species. ISME J. 12 (9), 2142–2151.

Liu, Y., Kim, H., Franklin, R., Bond, D.R., 2010. Gold line array electrodes increase substrate affinity and current density of electricity-producing *G. sulfurreducens* biofilms. Energy Environ. Sci. 3 (11), 1782–1788.

Logan, B.E., 2009. Exoelectrogenic bacteria that power microbial fuel cells. Nat. Rev. Microbiol. 7 (5), 375–381.

Logan, B.E., Regan, J.M., 2006. Microbial fuel cells - challenges and applications. Environ. Sci. Technol. 40 (17), 5172–5180.

Malvankar, N.S., Tuominen, M.T., Lovley, D.R., 2012. Biofilm conductivity is a decisive variable for high-current-density *Geobacter sulfurreducens* microbial fuel cells. Energy Environ. Sci. 5 (2), 5790–5797.

Malvankar, N.S., Vargas, M., Nevin, K.P., Franks, A.E., Leang, C., Kim, B.-C., Inoue, K., Mester, T., Covalla, S.F., Johnson, J.P., Rotello, V.M., Tuominen, M.T., Lovley, D.R., 2011. Tunable metallic-like conductivity in microbial nanowire networks. Nat. Nanotechnol. 6 (9), 573–579.

Marsili, E., Sun, J., Bond, D.R., 2010. Voltammetry and growth physiology of *Geobacter sulfurreducens* biofilms as a function of growth stage and imposed electrode potential. Electroanalysis 22 (7-8), 865–874.

McGlynn, S.E., Chadwick, G.L., Kempes, C.P., Orphan, V.J., 2015. Single cell activity reveals direct electron transfer in methanotrophic consortia. Nature 526 (7574), 531–535.

Nakamura, R., Ishii, K., Hashimoto, K., 2009. Electronic absorption spectra and redox properties of C type cytochromes in living microbes. Angew. Chem. Int. Ed. 48 (9), 1606–1608.

Nevin, K.P., Kim, B.-C., Glaven, R.H., Johnson, J.P., Woodard, T.L., Methé, B.A., DiDonato Jr., R.J., Covalla, S.F., Franks, A.E., Liu, A., Lovley, D.R., 2009. Anode biofilm transcriptomics reveals outer surface components essential for high density current production in *Geobacter sulfurreducens* fuel cells. PLoS One 4 (5), e5628.

Nevin, K.P., Richter, H., Covalla, S.F., Johnson, J.P., Woodard, T.L., Orloff, A.L., Jia, H., Zhang, M., Lovley, D.R., 2008. Power output and columbic efficiencies from biofilms of *Geobacter sulfurreducens* comparable to mixed community microbial fuel cells. Environ. Microbiol. 10 (10), 2505–2514.

Reguera, G., Nevin, K.P., Nicoll, J.S., Covalla, S.F., Woodard, T.L., Lovley, D.R., 2006. Biofilm and nanowire production leads to increased current in *Geobacter sulfurreducens* fuel cells. Appl. Environ. Microbiol. 72 (11), 7345–7348.

Reguera, G., Pollina, R.B., Nicoll, J.S., Lovley, D.R., 2007. Possible nonconductive role of *Geobacter sulfurreducens* pilus nanowires in biofilm formation. J. Bacteriol. 189 (5), 2125–2127.

Renslow, R.S., Babauta, J.T., Dohnalkova, A.C., Boyanov, M.I., Kemner, K.M., Majors, P. D., Fredrickson, J.K., Beyenal, H., 2013. Metabolic spatial variability in electrode-respiring *Geobacter sulfurreducens* biofilms. Energy Environ. Sci. 6 (6), 1827–1836.

Richter, H., Nevin, K.P., Jia, H.F., Lowy, D.A., Lovley, D.R., Tender, L.M., 2009. Cyclic voltammetry of biofilms of wild type and mutant Geobacter sulfurreducens on fuel cell anodes indicates possible roles of OmcB, OmcZ, type IV pili, and protons in extracellular electron transfer. Energy Environ. Sci. 2 (5), 506.

Robuschi, L., Tomba, J.P., Schrott, G.D., Bonanni, P.S., Desimone, P.M., Busalmen, J.P., 2013. Spectroscopic slicing to reveal internal redox gradients in electricity-producing biofilms. Angew. Chem. Int. Ed. 52 (3), 925–928.

Rollefson, J.B., Stephen, C.S., Tien, M., Bond, D.R., 2011. Identification of an extracellular polysaccharide network essential for cytochrome anchoring and biofilm formation in *Geobacter sulfurreducens*. J. Bacteriol. 193 (5), 1023–1033.

Seeliger, S., Cord-Ruwisch, R., Schink, B., 1998. A periplasmic and extracellular c-type cytochrome of *Geobacter sulfurreducens* acts as a ferric iron reductase and as an electron carrier to other acceptors or to partner bacteria. J. Bacteriol. 180 (14), 3686–3691.

Serra, D.O., Richter, A.M., Klauck, G., Mika, F., Hengge, R., 2013. Microanatomy at cellular resolution and spatial order of physiological differentiation in a bacterial biofilm. mBio 4 (2) e00103-00113.

Snider, R.M., Strycharz-Glaven, S.M., Tsoi, S.D., Erickson, J.S., Tender, L.M., 2012. Long-range electron transport in *Geobacter sulfurreducens* biofilms is redox gradient-driven. Proc. Natl. Acad. Sci. U.S.A. 109 (38), 15467–15472.

Steidl, R.J., Lampa-Pastirk, S., Reguera, G., 2016. Mechanistic stratification in electroactive biofilms of *Geobacter sulfurreducens* mediated by pilus nanowires. Nat. Commun. 7, 12217.

Stephen, C.S., LaBelle, E.V., Brantley, S.L., Bond, D.R., 2014. Abundance of the multiheme c-type cytochrome OmcB increases in outer biofilm layers of electrode-grown *Geobacter sulfurreducens*. PLoS One 9 (8), e104336.

Strycharz-Glaven, S.M., Snider, R.M., Guiseppi-Elie, A., Tender, L.M., 2011. On the electrical conductivity of microbial nanowires and biofilms. Energy Environ. Sci. 4 (11), 4366–4379.

Strycharz, S.M., Malanoski, A.P., Snider, R.M., Yi, H., Lovley, D.R., Tender, L.M., 2011. Application of cyclic voltammetry to investigate enhanced catalytic current generation by biofilm-modified anodes of *Geobacter sulfurreducens* strain DL1 vs. variant strain KN400. Energy Environ. Sci. 4 (3), 896–913.

Sun, D., Cheng, S., Wang, A., Li, F., Logan, B.E., Cen, K., 2015. Temporal-spatial changes in viabilities and electrochemical properties of anode biofilms. Environ. Sci. Technol. 49 (8), 5227–5235.

Sun, M., Li, W.-W., Yu, H.-Q., Harada, H., 2012. A novel integrated approach to quantitatively evaluate the efficiency of extracellular polymeric substances (EPS) extraction process. Appl. Microbiol. Biotechnol. 96 (6), 1577–1585.

Sure, S., Ackland, M.L., Torriero, A.A.J., Adholeya, A., Kochar, M., 2016. Microbial nanowires: an electrifying tale. Microbiology 162 (12), 2017–2028.

Tan, Y., Adhikari, R.Y., Malvankar, N.S., Ward, J.E., Woodard, T.L., Nevin, K.P., Lovley, D.R., 2017. Expressing the *Geobacter metallireducens* PilA in *Geobacter sulfurreducens* yields pili with exceptional conductivity. mBio 8 (1) e02203-02216.

Thomas, P.E., Ryan, D., Levin, W., 1976. An improved staining procedure for the detection of the peroxidase activity of cytochrome P-450 on sodium dodecyl sulfate polyacrylamide gels. Anal. Biochem. 75 (1), 168–176.

Torres, C.I., Krajmalnik-Brown, R., Parameswaran, P., Marcus, A.K., Wanger, G., Gorby, Y.A., Rittmann, B.E., 2009. Selecting anode-respiring bacteria based on anode potential: phylogenetic, electrochemical, and microscopic characterization. Environ. Sci. Technol. 43 (24), 9519–9524.

Torres, C.I., Lee, H.-S., Rittmann, B.E., 2008. Carbonate species as OH^- carriers for decreasing the pH gradient between cathode and anode in biological fuel cells. Environ. Sci. Technol. 42 (23), 8773–8777.

Ueki, T., Leang, C., Inoue, K., Lovley, D.R., 2012. Identification of multi-component His-Asp phosphorelay system controlling flagella and motility gene expression in *Geobacter* species. J. Biol. Chem. 287 (14), 10958–10966.

Vargas, M., Malvankar, N.S., Tremblay, P.-L., Leang, C., Smith, J.A., Patel, P., Synoeyenbos-West, O., Nevin, K.P., Lovley, D.R., 2013. Aromatic amino acids required for pili conductivity and long-range extracellular electron transport in *Geobacter sulfurreducensp*. mBio 4 (2) e00105-00113.

Wang, F., Gu, Y., O'Brien, J.P., Yi, S.M., Yalcin, S.E., Srikanth, V., Shen, C., Vu, D., Ing, N. L., Hochbaum, A.I., Egelman, E.H., Malvankar, N.S., 2019. Structure of microbial nanowires reveals stacked hemes that transport electrons over micrometers. Cell 177 (2), 361–369 e310.

Ye, J., Hu, A., Ren, G., Chen, M., Tang, J., Zhang, P., Zhou, S., He, Z., 2018. Enhancing sludge methanogenesis with improved redox activity of extracellular polymeric substances by hematite in red mud. Water Res. 134, 54–62.

Yi, H., Nevin, K.P., Kim, B.-C., Franks, A.E., Klimes, A., Tender, L.M., Lovley, D.R., 2009. Selection of a variant of *Geobacter sulfurreducens* with enhanced capacity for current production in microbial fuel cells. Biosens. Bioelectron. 24 (12), 3498–3503.